0026-895X/97/061042-11$3.00/0

MOLECULAR PHARMACOLOGY, **51:**1042–1052 (1997).

Purification of a New Dimeric Protein from *Cliona vastifica* Sponge, which Specifically Blocks a Non-L-Type Calcium Channel in Mouse Duodenal Myocytes

JEAN-LUC MOREL, HERVÉ DROBECQ, PIERRE SAUTIERE, ANDRÉ TARTAR, JEAN MIRONNEAU, JANTI QAR, JEAN-LOUIS LAVIE, and MICHEL HUGUES

Centre National de la Recherche Scientifique Enseignement Supérieur Associé 5017, Physiopathologie et Pharmacologie Vasculaire, Faculté de Pharmacie, Université de Bordeaux II, 33076 Bordeaux, France (J.-L.M., J.M., J.-L.L., M.H.), Institut Pasteur de Lille, Service de Chimie des Biomolécules, 59019 Lille, France (H.D., P.S., A.T.), and Department of Biological Science, Faculty of Sciences, Yarmouk University, Irbid, Jordan (J.Q.)

Received December 20, 1996; Accepted March 10, 1997

SUMMARY

Marine sponges are synthesizing a wide variety of peptidic and organic molecules with biological activities. Multiple-step purification of *Cliona vastifica* extract led to a new dimeric peptide (mapacalcine; M_r = 19,064) that is composed of two homologous chains, each containing nine cysteins. This protein has been found to selectively block a new calcium conductance characterized in mouse duodenal myocytes with an IC_{50} value of ~0.2 μM. The mapacalcine-sensitive current was a non-L-type calcium current activated from a holding potential of −80 mV that persisted during stimulation of the cell at high frequencies (0.1–0.2 Hz) within 5–10 min. Time constants of inactivation were similar for both L-type and non-L-type calcium currents. The non-L-type calcium current of duodenal myocytes was not blocked by the pharmacological agents specific for N-, L-, P-, or Q-type calcium channels. Mapacalcine was unable to block T-type calcium current in portal vein myocytes as well as voltage-dependent potassium currents and calcium-activated chloride currents in duodenal and portal vein cells. Mapacalcine did not affect caffeine-induced calcium responses, indicating that it did not interfere with intracellular calcium stores. Competition experiments on mouse intestinal membranes showed that mapacalcine did not interact with dihydropyridines receptors. These data suggest that mapacalcine may be a specific inhibitor of a new type of calcium current, first identified in duodenal myocytes.

Natural peptides have been invaluable tools for pharmacological and biochemical investigations of a wide range of physiological functions (1). Calcium channels have been investigated in large part because of the existence of a great number of molecules acting on these channels. They have been classified according to their electrophysiological and pharmacological properties (2, 3) and represent an important family of ionic channels because they are directly acting on calcium homeostasis of the cell. Biological functions such as muscle contraction, hormone secretion, or neurotransmitter release are directly dependent on intracellular calcium variations. These channels are involved in a wide range of pathologies, including cardiovascular system diseases (4, 5). Different types of calcium channels can be expressed in the same cellular type (6–8). L- and T-type calcium channels are, for example, found in most excitable cells, although the physiological role of the T-type channel remains unclear. The L-type channel is mainly involved in excitation/contraction or excitation/secretion couplings and is sensitive to dihydropyridines, a class of calcium antagonists widely used in the treatment of cardiovascular pathologies. L- and T-type calcium channels are also present in smooth muscle cells (6, 7). Interestingly, several types of voltage-dependent calcium channels have been described in gastrointestinal smooth muscles (9, 10). P-type channels are mainly found in Purkinje cells and are sensitive to a spider toxin, the ω-agatoxin IVA (11, 12). N-type channels are present on a wide variety of neurons and are blocked by ω-conotoxin GVIA (13). Both P- and N-type calcium channels play an important role in the control of neurotransmitters release (12, 14). Another type of calcium channel that presents with similarities to the P-type channel is the Q-type; it has been described in the granular layer of cerebellum. It could be involved in synaptic transmission between neurons from CA3 and CA1 layers in hippocampus and is sensitive to ω-conotoxin MVII C (15). Genetic investigations demonstrated the existence of several

This work was supported by grants from the Fondation pour la Recherche Médicale, Pôle Médicament Aquitaine, and Région Aquitaine France.

ABBREVIATIONS: HPLC, high performance liquid chromatography; EGTA, ethylene glycol bis(α-aminoethyl ether)-*N*,*N*,*N*′,*N*′-tetraacetic acid; HEPES, 4-(2-hydroxyethyl)-1-piperazineethanesulfonic acid; TFA, trifluoroacetic acid.

genes encoding for a same $\alpha 1$ subunit (16). This phenomenon could be responsible for the functional differences observed for a same channel type expressed in different cell types. The actual situation seems to be complex because there are many calcium channel subtypes for which functional and biological properties remain unclear, in part because of the absence of a consequent pharmacology (3). Marine sponges are known to synthesize many organic and peptidic molecules with interesting biological properties; for example, latrunculin A interacts with actin polymerization (17). Peptides from Bahamian sponge, discobahamin A and B, or halicylindramides from *Halichondria cylindrata* have antifungal properties (18, 19). Protease inhibitory peptides are also found in marine sponge (20). Many other peptides with biological activity have been isolated from sponges, but as far as we know, no calcium channel effectors have been described until now. A previous report has shown that sponge extracts are able to block carbachol-induced contractions in intestinal smooth muscle, which are insensitive to dihydropyridines (21). These observations suggest that these organisms could synthesize calcium channel effectors. In this work, we describe, on the one hand, the existence of both L-type and non-L-type calcium currents in mouse duodenal smooth muscle cells. The non-L-type calcium current is insensitive to a variety of calcium channel blockers. On the other hand, we describe the purification and sequence of a dimeric protein (mapacalcine) isolated from *C. vastifica* sponge that is able to specifically block the duodenal non-L-type calcium current, suggesting the existence of a new class of calcium channels.

Materials and Methods

***C. vastifica* extraction and purification.** The sponges (*C. vastifica*) were collected from the Red Sea or obtained from Latoxan (Rosans, France). The entire sponge and its stony substrate were ground and soaked in 50% ethanol for 24 hr. The ethanol was then evaporated in a Rota Vapor concentrator (Bioblock, Illkirsh, France) and the aqueous phase was lyophilized. The powder obtained was stored at −20° until use.

Gel filtration chromatography. Typical purification was performed using 2 g of powder that was resuspended in 15 ml of 1% acetic acid and centrifuged for 1 hr at 140,000 × *g*. The supernatant was loaded onto a Sephadex G50 (fine) column (2.5 × 100 cm) equilibrated with 1% acetic acid. The column was then eluted at a rate of 0.7 ml/min for 12 hr. Then, 15-ml fractions were collected, and the elution was monitored by absorbance measurement at 280 nm. All subsequent purification steps were performed with HPLC.

Ion exchange chromatography. The active fractions obtained from gel filtration were loaded onto a TSK gel SP-5PW column (2.1 × 15 cm; Toyo Soda, Tokyo, Japan) equilibrated with 1% acetic acid (buffer A). The column was then washed at a rate of 8 ml/min for 10 min with buffer A and eluted by a gradient of 0–100% 1 M ammonium acetate (buffer B) during 100 min. Fractions were collected every 2 min. Elution was followed by on-line absorbance recording at 280 nm.

Reverse-phase purification step. Selected fractions from ion exchange chromatography underwent a purification step on a reverse-phase C 8 column (Lichrosorb 100 RP 8, Merck, Nogent sur Marne, France; 10 × 250 mm) equilibrated with water containing 0.1% TFA (buffer A) at 3 ml/min. The column was washed 10 min with buffer A; then, elution was performed by a gradient of 0–80% acetonitrile containing 0.1% TFA over 40 min. One-minute fractions were collected, and the chromatogram was recorded at 280 nm.

Desalting operation. Before being tested by electrophysiological techniques, fractions obtained from gel filtration or ion exchange steps were desalted using SepPak cartridges (Waters, Milford, MA). The cartridge was previously washed by 5 ml of acetonitrile and then rinsed with 10 ml of 0.1% TFA in water. Samples to be desalted were mixed with TFA (final concentration, 0.1%) and loaded onto the cartridge. After washing with 10 ml of 0.1% TFA in water, the retained material was eluted by 1 ml of water/acetonitrile (50:50) and 1 ml of acetonitrile, both containing 0.1% TFA. The elutates were evaporated using a Christ concentrator (Bioblock), and the desalted material obtained was used for electrophysiology.

Sequence analysis. The purity of the toxin obtained after reverse-phase HPLC purification was assessed by the use of capillary electrophoresis (270A-HT Capillary Electrophoresis System; Applied Biosystems, Norwalk, CT) in 20 mM sodium citrate buffer, pH 2.5, at 30 kV and 30° for 10 min with a 50-cm, 50-μm-diameter capillary. UV detection was performed at 200 nm.

Amino acid analysis. Amino acid analyses were performed with a Beckman Instruments (Palo Alto, CA) 6300 amino acid analyzer after hydrolysis in 6 M HCl (Pierce Chemical, Rockford, IL) in the presence of 0.25% phenol at 110° in sealed/evacuated tubes for 24, 48, and 72 hr.

Reduction and carboxamidoethylation. The toxin (0.4 mg, ~20 nmol) was dissolved in 100 μl of 0.1 M ammonium bicarbonate buffer, pH 8.0, containing 6 M guanidium chloride and 0.1 M dithiothreitol and maintained at 70° for 30 min. The mixture was then brought to room temperature, and alkylation of the reduced toxin was performed for 45 min by the addition of 50 μl of 6 M acrylamide in water. The carboxamidoethylated toxin was desalted by reverse-phase HPLC on a C18 Vydac column (200 × 2.1 mm, 5-μm particle size, 300-Å pore diameter) at a flow rate of 100 μl/min. After washing out the salts with 0.05% TFA, the protein was eluted with 80% acetonitrile in 0.05% TFA. The elution was monitored at 210 nm. The carboxamidoethylated toxin (0.1 mg, ~10 nmol) dissolved in 100 μl of 0.1 M ammonium bicarbonate, pH 8.0, was then hydrolyzed for 2 hr at 37° with $TosPheCH_2Cl$-treated trypsin using an enzyme-to-substrate ratio of 1:100 (w/w).

Peptide separation. The tryptic peptides were separated by reverse-phase HPLC on a C18 Vydac column (200 × 2.1 mm, 5-μm particle size, 300-Å pore diameter) using a gradient of acetonitrile of 8–40% in 0.05% TFA for 90 min at a flow rate of 100 μl/min. Elution of peptides was monitored by UV absorption at 210 nm.

Ion spray mass spectrometry. The molecular mass of the native toxin and that of its carboxamidoethylated derivative were determined by ion spray mass spectrometry. Samples (10–20 pmol/μl) were dissolved in 20% acetonitrile in water/formic 0.1% acid. Ion spray mass spectra were recorded on a simple quadrupole mass spectrometer (API I; Perkin-Elmer Cetus, Norwalk, CT) equipped with an ion-spray (nebulizer-assisted electrospray) source (Sciex, Toronto, Ontario, Canada). The solutions were continuously infused with a medical infusion pump (model 11; Harward Apparatus, South Natick, MA) at a flow rate of 5 μl/min.

Polypropylene glycol was used to calibrate the quadrupole. Ion spray mass spectra were acquired at unit resolution by scanning m/z 1200–2400 with a step size of 0.1 Da and a dwell time of 2 msec. Five to 10 spectra were summed. The potential of the spray needle was held at +5 kV. Spectra were recorded at an orifice voltage of +90 V.

We used Mac BIO Spec software (Sciex) for calculation of the molecular masses of the samples.

Sequence analysis. Sequencing of protein in native form or after reduction and carboxamidoethylation of cysteines and of tryptic peptides was carried out on a gas-phase sequencer (model 470A, Applied Biosystems) using the 03RPTH program. Phenylthiohydantoin derivatives of amino acids were identified with an on-line phenylthiohydantoin amino acid analyzer (model 120A, Applied Biosystems).

Cell preparation. Swiss mice (20–25 g) and Wistar rats (150–160 g) were stunned and then killed by cervical dislocation. The longitudinal layer of the mouse duodenal smooth muscle (or the rat portal vein) was cut into several pieces and incubated for 10 min in a low-Ca^{2+} (40 μM) physiological solution. Then, 0.8 mg/ml collage-

nase, 0.2 mg/ml pronase E, and 1 mg/ml bovine serum albumin were added, and the mixture was maintained at 37° for 20 min. The solution was then renewed, and the pieces of mouse duodenum (or rat portal vein) were incubated under the same conditions for an additional 20-min period. Tissues were then placed in enzyme-free solution and dissociated using a fire-polished Pasteur pipette to release cells. Cells were maintained in short term primary culture in Medium 199 containing 10% fetal calf serum (duodenum) or 5% fetal calf serum (portal vein), 1 mM glutamine, 1 mM pyruvate, 20 units/ml penicillin, and 20 μg/ml streptomycin. Cells were maintained in culture at 37° in an incubator under controlled atmosphere (5% CO_2) and used for electrophysiology within 36 hr.

Patch-clamp measurements. Voltage-clamp and membrane current recordings were made with a standard patch-clamp technique using a List EPC-7 patch-clamp amplifier (List Electronics, Darmstadt, Germany). The whole-cell recording mode was performed with patch pipettes of 1–3 MΩ resistance. Membrane potential and current records were stored and analyzed using an IBM-PC computer (pClamp system).

Fluorescence measurements. Whole-cell membrane currents and intracellular calcium concentration were measured simultaneously as previously reported (22). Briefly, 50 μM Indo-1 was added to the pipette solution and entered into the cells after establishment of the whole-cell recording mode. Indo-1 repartition was usually homogeneous over the cytoplasm, and no compartmentalization of the dye was observed. Cells were mounted in a perfusion chamber and placed on the stage of an inverted microscope (Nikon Diaphot). The cell studied was illuminated at 360 nm. Emitted light from a window slightly larger than the cell was counted simultaneously at 405 and 480 nm by two photomultipliers (P_1, Nikon). Intracellular calcium concentration was estimated on the basis of the 405 nm/480 nm ratio using a calibration for Indo-1 determined within cells. Some experiments were carried out in the presence of 1 μM oxodipine (a light-stable dihydropyridine derivative) to inhibit L-type voltage-dependent calcium channels. All measurements were made at 25 ± 1°.

Solutions. The normal physiological solution contained 30 mM NaCl, 5.6 mM KCl, 1 mM $MgCl_2$, 2 mM $CaCl_2$, 11 mM glucose, and 10 mM HEPES/NaOH, pH 7.4. The basic pipette solution contained 130 mM CsCl and 10 mM HEPES/CsOH, pH 7.3. For calcium current recordings, CsCl was used instead of KCl in the pipette and external solutions to block outward potassium currents. In addition, 10 mM EGTA, 5 mM Na_2ATP, and 1 mM $MgCl_2$ were added to the basic pipette solution. For potassium channel current recordings, KCl was used in the external and pipette solutions. Caffeine, *C. vastifica* toxin, and all pharmacological agents were applied to the recorded cell by pressure ejection from a glass pipette for the period indicated on the records. Before each experiment, an application of physiological solution alone was tested, and cells with movement artifacts were excluded. In addition, *C. vastifica* toxin and all pharmacological agents were tested by their addition to the perfusion solution.

Intestinal membrane preparation. Mice were killed by cervical dislocation. Small intestines were removed and rinsed with ice-cold buffer containing 140 mM NaCl, 20 mM Tris·HCl, pH 7.4, and 0.1 mM phenylmethylsulfonyl fluoride (washing buffer). The intestines were then opened and scraped to remove the epithelial cell layer. Intestinal smooth muscles were diluted 10-fold (w/v) with the washing buffer at 4° and homogenized 30 sec in a Warring Blender and then twice at 30 sec with a Polytron homogenizer. Homogenate was centrifuged at 4000 × *g* for 7 min, and the supernatant was centrifuged for 45 min at 140,000 × *g*. All centrifugation steps were performed at 4°. The pellets were resuspended in the washing buffer and frozen at −80° until use. Proteins were measured using BioRad (Hercules, CA) protein assay reagent and lysozyme as standard.

Binding of [^{3}H]-(+)-isradipine. Intestinal membranes (0.5 mg of protein/ml) were incubated at 25° in 0.1% bovine serum albumin and 20 mM HEPES/NaOH, pH 7.4, in the presence of 100 pM labeled (+)-isradipine and increasing concentrations of unlabeled isradipine, oxodipine, and mapacalcine. After a 1-hr incubation, 0.8-ml aliquots were filtered through Whatman GF/C filters and washed three times with 0.1 M ice-cold Tris/Cl buffer, pH 7.4. Radioactivity retained on the filters was estimated with a Packard scintillation counter (Meriden, CT).

Chemicals and drugs. All reagents and solvents were of the highest purity available. Collagenase (E.C. 3.4.24.3) and trypsin (E.C. 3.4.21.4) treated with $TosPheCH_2Cl$ were from Worthington (Freehold, NJ). Carboxypeptidase P sequencing grade (E.C. 3.4.16.1) was purchased from Boehringer-Mannheim Biochemica (Mannheim, Germany). Pronase (E.C. 3.4.24.31), bovine serum albumin, tetrodotoxin, and amiloride were from Sigma Chemical (St. Louis, MO). ω-Conotoxin GVIA, ω-agatoxin IVA, and ω-conotoxin MVII C were from Latoxan (Rosans, France). Fenoverine was from Delalande (Paris, France). Diltiazem was from Synthelabo (Paris, France). Desmethoxyverapamil was from Knoll (Ludwigshafen, Germany). Isradipine was from Sandoz (Rueil-Malmaison, France). Medium 199 was from Flow Laboratories (Puteaux, France). Fetal bovine serum was from Flobio (Courbevoie, France). Streptomycin, penicillin, glutamine, and pyruvate were from GIBCO (Paisley, UK). Oxodipine was a gift from Dr. A. Galiano (IQB, Madrid, Spain). Caffeine and HEPES were from Merck. Indo-1 was from Calbiochem (Meudon, France).

Data analysis. The results are expressed as mean ± standard error. Significance was tested with the Student's *t* test. Values of $p < 0.05$ were considered statistically significant. Inhibition and concentration-response curves were analyzed by a nonlinear least-squares fitting program according to models involving one or two binding sites.

Results

Calcium currents in duodenal myocytes. With CsCl in the pipette and bathing solutions to inhibit potassium currents, depolarizing pulses were applied from two holding potentials (−80 or −60 mV) to 0 mV for 150 msec at 0.05 Hz. With 2 mM $CaCl_2$, the inward current obtained from a holding potential of −80 mV was larger than that obtained from a holding potential of −60 mV (Fig. 1A). Decay of the calcium currents elicited from −60 and −80 mV was well fitted with a two-exponential function. For inward currents evoked by depolarizations to 0 mV, the time constants of inactivation were 18 ± 5 and 96 ± 29 msec for the current elicited from −60 mV (12 experiments) and 12 ± 2 and 81 ± 21 msec for the current elicited from −80 mV (18 experiments). The effects of several compounds that inhibit calcium channels were tested on the maximal calcium currents elicited from the two holding potentials. As shown in Table 1, the maximal calcium current elicited from −60 mV was suppressed by isradipine, oxodipine, fenoverine, diltiazem, and desmethoxyverapamil. In contrast, when the cells were held at −80 mV, high concentrations of these compounds inhibited the calcium current by only 40–50%, suggesting that a component of inward current resistant to calcium channel antagonists was unmasked by negative holding potentials.

A common method of separating L-type calcium current from other calcium currents is to dialyze the cell sufficiently long to obtain the removal of the L-type calcium current. At high stimulation frequency (0.1 Hz), the L-type calcium current elicited from −60 mV subsided quickly within 5–6 min (Fig. 1B). When the holding potential was returned to −80 mV, inward currents were recorded for 10–15 min at the same stimulation frequency without significant modification of their time course (Fig. 1C). In addition, this current was insensitive to high concentrations of isradipine (10–50 μM, 21

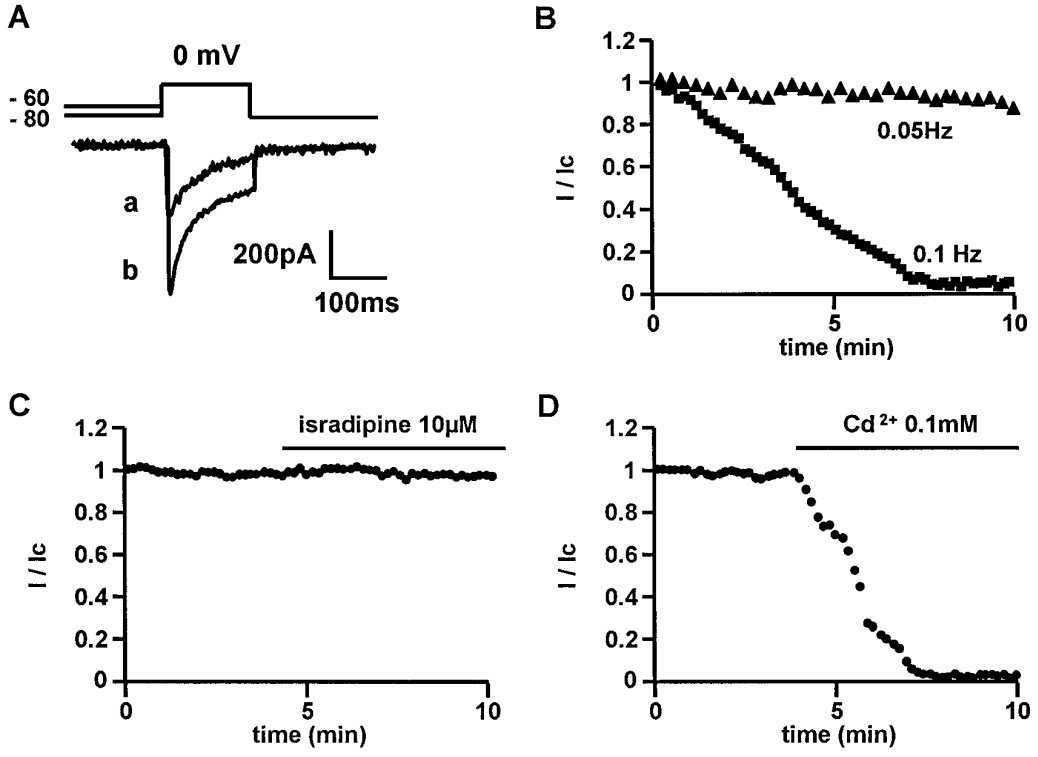

Fig. 1. Calcium currents in mouse duodenal myocytes. A, Currents elicited from holding potentials of (*a*) −60 mV and (*b*) −80 mV to 0 mV with 2 mM $CaCl_2$ in the external solution. B, Time course of calcium currents elicited from a holding potential of −60 to 0 mV at stimulation frequencies of (▲) 0.05 Hz and (■) 0.1 Hz. C, Effect of 10 μM isradipine on the calcium current elicited by depolarizing steps from −80 to 0 mV at a stimulation frequency of 0.1 Hz. D, Effect of 0.1 mM Cd^{2+} on the calcium current elicited by depolarization steps from −80 to 0 mV at a stimulation frequency of 0.1 Hz. Calcium current was expressed as a fraction of control current (I/I_c) obtained 3 min after the membrane was ruptured under the pipette.

TABLE 1

Inhibition of maximal Ca^{2+} currents evoked by depolarizing pulses from holding potentials (h) of −60 or −80 mV

Value represents the inhibition percentage of Ca^{2+} current [$(I/I_c) - 1 \times 100$], in which I_c is the control current in the absence of drug and I is the current in the presence of drug for 5 min. Values are mean ± standard error of *n* experiments.

Depolarization (holding potential/pulse)	−60/+10 mV	−80/0 mV
Isradipine (10 μM)	−94 ± 6% (*n*= 7)	−43 ± 9% (*n*=13)
Oxodipine (10 μM)	−96 ± 3% (*n*=12)	−36 ± 6% (*n*= 9)
Fenoverine (10 μM)	−90 ± 7% (*n*= 9)	−43 ± 6% (*n*=11)
Diltiazem (10 μM)	−90 ± 7% (*n*= 6)	−54 ± 11% (*n*= 7)
Desmethoxyverapamil (5 μM)	−93 ± 6% (*n*= 6)	−53 ± 10% (*n*=10)

experiments), ω-conotoxin GVIA (0.1–3 μM, nine experiments), ω-agatoxin IVA (0.1 μM, seven experiments), ω-conotoxin MVIIC (10 μM, 10 experiments), amiloride (10 μM, five experiments), and tetrodotoxin (0.1–10 μM, nine experiments). However, this current was blocked by 0.1 mM Cd^{2+} (Fig. 1D) or 1 mM Ni^{2+} (data not shown). Fig. 2 illustrates the current-voltage relationships of the two types of currents. The calcium current elicited from a holding potential of −60 mV, at a stimulation frequency of 0.05 Hz, had a threshold for activation of ~−35 mV and generated a maximal current at +10 mV (Fig. 2A). The calcium current elicited from a holding potential of −80 mV, at a stimulation frequency of 0.1 Hz for 10 min (▲) or in the presence of 10 μM oxodipine (■), was activated from a more negative threshold of ~−45 mV and reached a maximum value at 0 mV (Fig. 2B). Both currents had an apparent reversal potential of ~+80 mV. The inactivation time constants of the oxodipine-resistant calcium current were estimated at various depolarizations. The fast time constants were steeply voltage dependent, whereas the slow time constants showed little variation with membrane potential (data not shown). Finally, the voltage-dependent inactivation of both calcium currents was examined with the two-pulse voltage-clamp protocol (Fig. 2C, *inset*). In this protocol, inactivation induced during a conditioning pulse (V_1) of 20-sec duration and a variable amplitude was estimated by the reduction in peak current associated with a test depolarization to 0 mV (V_2). The decrease of the test current was taken as an index of inactivation of the calcium current. Relative inactivation was expressed by plotting the test current versus the prepulse potential value. The amplitude of the test current was normalized to its value at the most negative prepulse (I/I_{max}). Fig. 2C shows that the relative inactivation of calcium current was progressively enhanced in the voltage range from −90 to −50 mV when obtained in the presence of 10 μM oxodipine or after 10 min of stimulation at 0.1 Hz. Half-maximal and complete inactivations of the non-L-type calcium current were obtained at membrane potentials of −70 ± 2 and −45 ± 5 mV (eight experiments), respectively. In contrast, the relative inactivation of the oxodipine-sensitive calcium current obtained from a holding potential of −60 mV was progressively enhanced in the voltage range from −60 to 0 mV. Half-maximal and complete inactivations of the L-type calcium current were obtained at membrane potentials of −40 ± 2 and −10 ± 3 mV (six experiments), respectively. Taken together, these results suggest that duodenal myocytes show two types of calcium currents, which can be separated by several experimental protocols.

***C. vastifica* extract purification and effects on calcium current.** A gel filtration (Sephadex G50) chromatogram is shown in Fig. 3A. Four pools were made with the fractions that were collected (P1–4). The different pools were desalted as described above and tested by the patch-clamp technique. Pool P3 (*arrows*) was found to inhibit the non-L-type calcium current elicited by depolarizations from −80 to 0 mV at a stimulation frequency of 0.1 Hz for 10 min and in

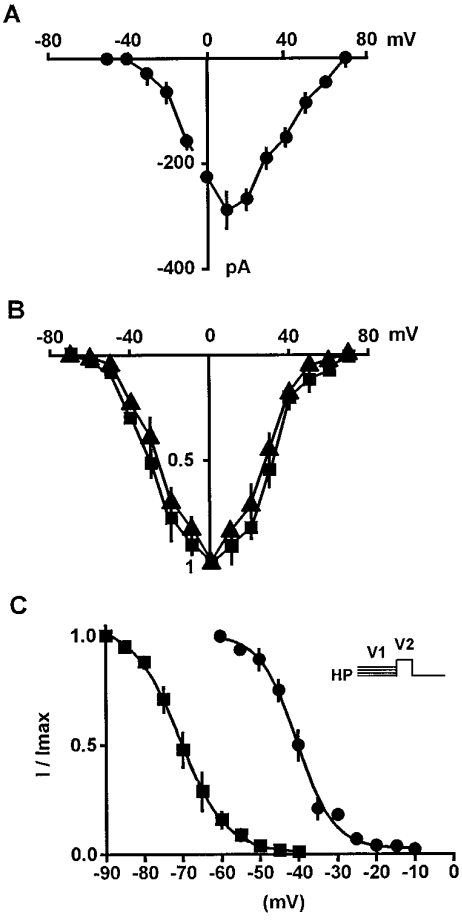

Fig. 2. Current-voltage relationships and steady state inactivation curves for the two types of calcium currents. A, Calcium currents elicited from a holding potential of −60 mV at a stimulation frequency of 0.05 Hz. B, Calcium currents elicited from a holding potential of −80 mV, (▲) at a stimulation frequency of 0.1 Hz for 10 min or (■) in the continuous presence of 10 μM oxodipine. Currents were expressed as a fraction of the peak current. C, Steady state inactivation curve obtained with the two-pulse protocol (*inset*) for the L-type calcium current from a holding potential of −60 mV (●) and for the non-L-type calcium current from a holding potential of −90 mV, after a 10-min period of stimulation frequency at 0.1 Hz (■). Data were fitted by curves of form $1/1[1 + \exp(V_m - V_h)/k]$, in which V_h is the potential at which half of current was inactivated, V_m is the membrane potential, and k is the slope factor. Calcium current was expressed as a fraction of maximal current (I/I_{max}). *Points,* mean response of 5–15 cells with the standard error (*vertical lines*).

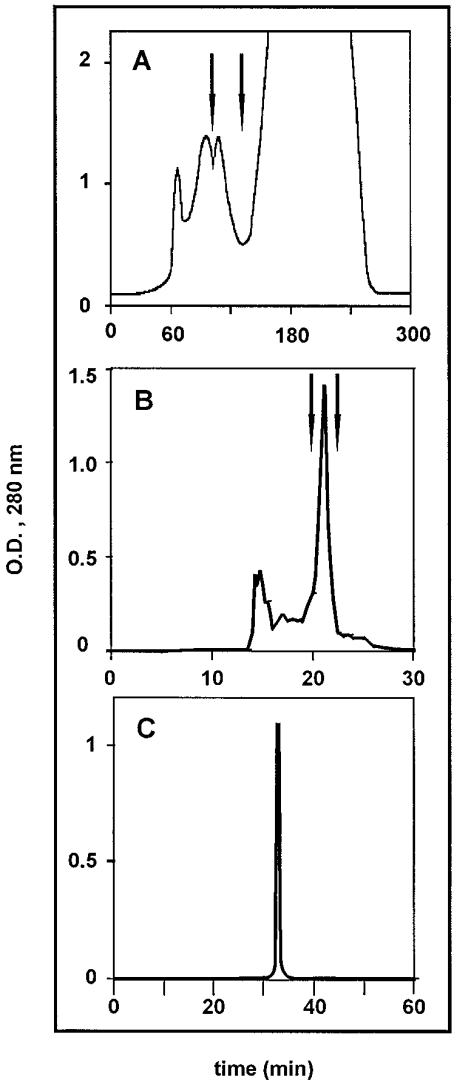

Fig. 3. Purification procedure of mapacalcine. A, The crude extract was centrifuged and loaded onto a Sephadex G50 (2.5 × 100 cm) column. Elution was performed at 0.7 ml/min with 1% acetic acid. The material shown eluting *between the arrows* contained the calcium channel-blocking activity. B, Ion exchange chromatography of the active material obtained from the Sephadex G50 purification step. The TSK gel SP-5PW column was eluted using a gradient from 0 to 1 M ammonium acetate over 100 min. The active material was eluted at 21–23 min (*arrows*). C, Reverse-phase chromatography of the active fraction obtained from the ion exchange step. Elution was performed at 3 ml/min on a reverse-phase C8 column (Lichrosorb 100 RP 8, Merck; 10 × 250 mm) by a gradient of 0–80% acetonitrile containing 0.1% TFA over 40 min. One symmetrical peak was eluted. and all the calcium channel-blocking activity was obtained under this peak. C, Material was sequenced and submitted to mass spectroscopy analysis before and after reduction and alkylation to demonstrate its dimeric structure. Data obtained demonstrated the presence of an homodimer (see Results).

the continuous presence of 10 μM oxodipine with an IC_{50} value of ~27 μg/ml. No variation of leak current and holding current was detected in the presence of *C. vastifica* extracts. Measurements were made only when the cell reached a steady state within 5–6 min. Pool P3 was loaded onto the TSK gel SP-5PW ion exchange column. The chromatogram that was obtained (Fig. 3B) shows, as expected, a multiple peak pattern. Different pools were collected and tested for calcium channel current inhibition after a desalting step. Inhibition of the calcium current was found under the peak eluted between 21 and 23 min under conditions used in Fig. 3B. No activity was detectable in the other fractions. The active fraction was named P3 C and loaded onto a C8 reverse-phase column. After elution of the C8 column, as described Materials and Methods, the chromatogram that was obtained (Fig. 3C) demonstrated the presence of a single symmetrical peak. The IC_{50} values obtained on the non-L-type calcium current varied from 5 ± 1 (5–12 experiments) to 3.6 ± 0.7 (5–15 experiments) μg/ml among the tested fractions. Electrophysiological experiments showed that all the calcium-blocking activity was eluted in this fraction; this peak was named P3 C3. At this stage, we submitted the material contained in P3 C3 to capillary electrophoresis analysis, and data showed that P3 C3 was homogeneous. The

TABLE 2

Amino acid composition of mapacalcine monomer

Results are expressed as number of residues/molecule of monomer and are the mean values from 24-, 48-, and 72-hr hydrolysates. Calculated mass (Da), 9,541.7; measured mass (Da), 19,063.9 ± 0.9.

Amino acid	Experimental value	Deduced value from established sequence
Asp	9.9	10
Thr	4.6	5
Ser	8.9	7
Glu	9.4	9
Pro	4.9	6
Gly	11.0	11
Ala	4.3	4
Cys	8.0	9
Val	4.0	4
Met	1.0	1
Ile	7.2	8
Leu	3.2	3
Tyr	4.9	5
Phe	2.1	2
His	1.7	2
Lys	1.2	1
Arg	2.2	2
Trp	N.D.	1
Total	89	

peptide (mapacalcine) was then submitted to sequence analysis.

Mapacalcine 3 primary structure. The amino acid composition of mapacalcine was mainly characterized by large amounts of dicarboxylic residues (21%), a significantly high content of glycine (12%) and cysteine (10%), and a low content of basic residues (5%; Table 2).

Native mapacalcine had a molecular mass of 19,063.9 ± 0.9 Da as measured by electrospray mass spectrometry, whereas the reduced and carboxamidoethylated mapacalcine had a molecular mass of 10,182.1 ± 0.9 Da. However, the mass calculated from the amino acid composition and sequence was 9,541.7 Da. These data clearly indicate that mapacalcine is indeed a homodimer with nine disulfide bridges. Furthermore, the carboxypeptidase P digestion of the reduced and carboxamidoethylated mapacalcine did not release any amino acid, leading us to conclude that the glutamine residue at the carboxyl terminus had an α-carboxamido group rather than an α-carboxylic group. This result was also supported by the mass spectrometry data, which showed a difference of two mass units between the measured mass and the calculated mass.

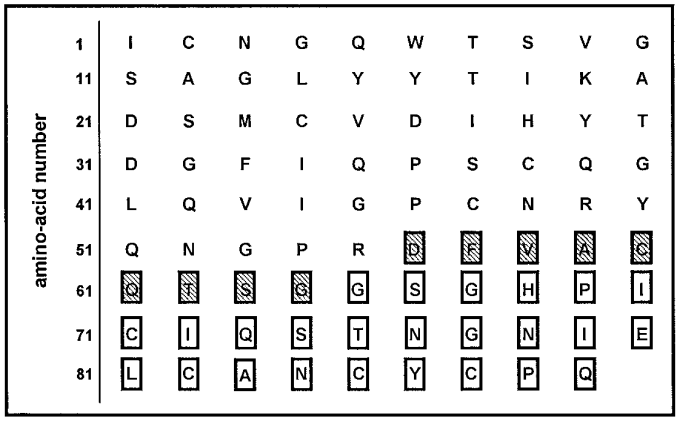

Fig. 4. Sequence of one chain of the dimer of mapacalcine. Methods used for the determination of the sequence are indicated as follows: *single letters*, residues identified by automated Edman degradation; *boxed letters*, peptide generated from cleavage of the reduced and carboxyethylated monomer with trypsin; *striped boxes*, residues identified by both direct Edman degradation and tryptic peptide sequencing.

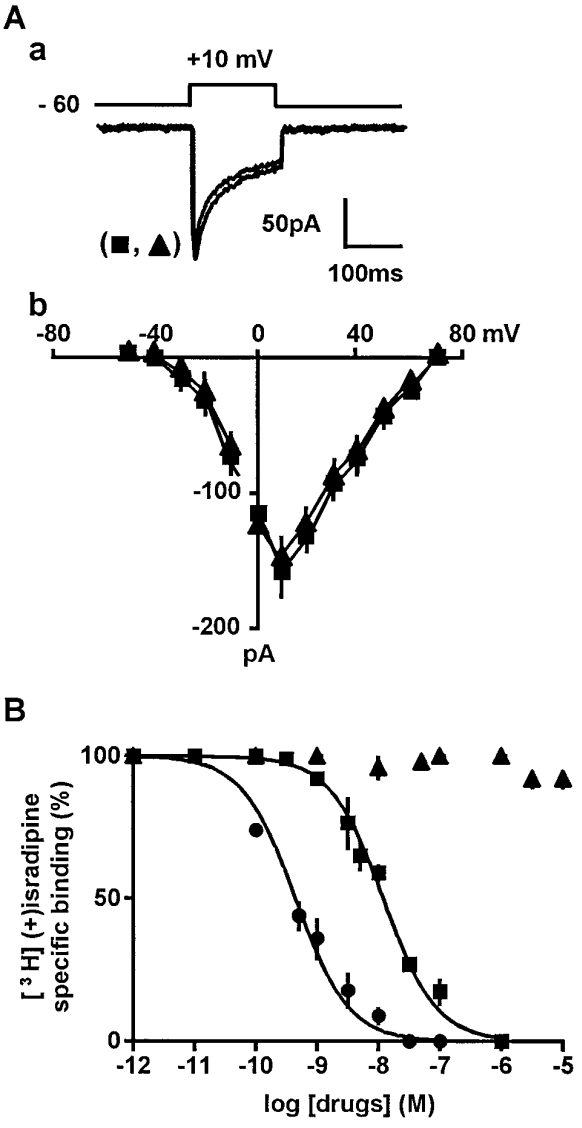

Fig. 5. Effects of mapacalcine on the L-type calcium current and [^{3}H]-(+)-isradipine binding. A, Calcium currents elicited from a holding potential of −60 mV at a stimulation frequency of 0.05 Hz in the (■) absence or (▲) presence of 5 μM mapacalcine for 5 min. *a*, Maximal calcium current. *b*, Current-voltage relationships. *Points,* mean of three to seven experiments, with the standard error shown (*vertical lines*). B, Competition experiments between [^{3}H]-(+)-isradipine, isradipine (●), oxodipine (■), and mapacalcine (▲). *Points,* mean response of four experiments, each carried out in duplicate, with the standard error shown (*vertical lines*). Nonspecific binding was not changed in the presence of the drugs.

The data obtained from automated Edman degradation of the carboxamidoethylated protein allowed the positive identification of the first 64 residues of the monomer. The remainder of the sequence was established by automated Edman degradation of the carboxyl-terminal tryptic peptide (residues 56–89) obtained by cleavage of the Arg—Asp bond with trypsin. The complete amino-acid sequence of the mapacalcine monomer is shown in Fig. 4.

Effects of mapacalcine on calcium currents. As shown in Fig. 5A, mapacalcine (1–5 μM) had no effect on the maximal L-type calcium current elicited by a depolarization from −60 to 0 mV, at a stimulation frequency of 0.05 Hz, in duodenal myocytes. There was no change in the voltage threshold, potential for the maximal current, or apparent reversal potential, as shown by the current-voltage relationships. The absence of effect of mapacalcine on L-type calcium channels was confirmed by study of the binding of [^{3}H]-(+)-isradipine to intestinal membranes (Fig. 5B). Inhibition of the high affinity [^{3}H]-(+)-isradipine binding was obtained with isradipine (K_i = 0.44 ± 0.04 nM, four experiments) and oxodipine (K_i = 12 ± 0.9 nM, four experiments). In contrast, mapacalcine (0.1 nM to 10 μM) had no effect on [^{3}H]-(+)-isradipine binding (four experiments).

Mapacalcine inhibited the calcium current elicited from −80 mV at a stimulation frequency of 0.1 Hz for 10 min and in the presence of 10 μM oxodipine (Fig. 6A). The inhibitory action of mapacalcine on this calcium current was observed in all the tested cells and was measured when the cells reached a steady state (i.e., within 5–6 min) (34 experiments). Typical inhibitory effects of 0.3 μM mapacalcine on the current-voltage relationship are shown in Fig. 6A. The maximal current was inhibited by 55 ± 7% (12 experiments) without any change in the voltage threshold, potential for the maximal current, and apparent reversal potential. The concentration-response curve shows that the concentration of mapacalcine required to reduce the non-L-type calcium current by 50% (IC_{50}) was 0.20 ± 0.03 μM (Fig. 6B). The Hill coefficient was estimated to be 0.8. The kinetics of calcium current inhibition by mapacalcine were obtained from three different concentrations (5, 0.5, and 0.05 μM). According to the equation of Weiland and Molinoff (23), both on- and off-rate constants were estimated, leading to an apparent dissociation constant of 0.4 μM. This value is in good agreement with the IC_{50} value (0.2 μM) obtained from the steady state concentration-response curve.

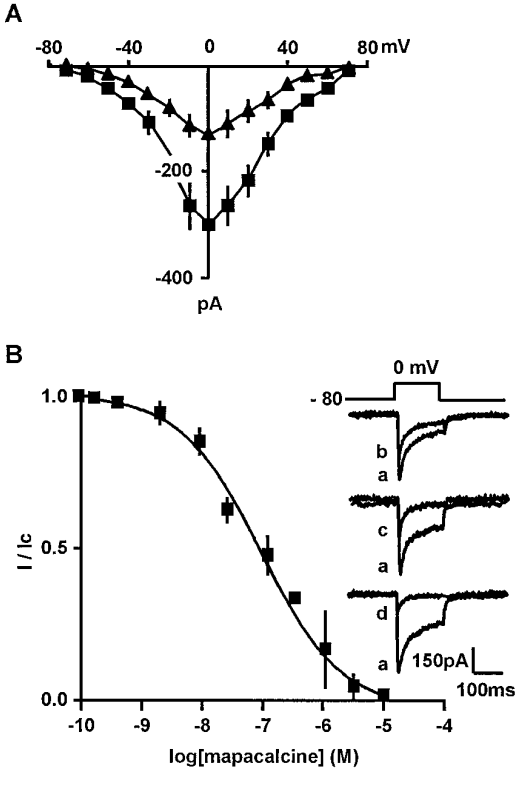

Fig. 6. Inhibitory effects of mapacalcine on the non-L-type calcium current in duodenal myocytes. Calcium currents were elicited from a holding potential of −80 mV at a stimulation frequency of 0.1 Hz and in the presence of 10 μM oxodipine. A, Current-voltage relationships in the (■) absence and (▲) presence of 0.3 μM mapacalcine for 5 min. B, Concentration-response relationship of the inhibitory action of mapacalcine. Calcium current was expressed as a fraction of control current in the absence of mapacalcine (I/I_c) and plotted against mapacalcine concentration. *Continuous line*, nonlinear regression of the data points assuming a Hill coefficient of 0.8. *Points,* mean response of 5–15 cells with the standard error shown (*vertical lines*). *Inset*, calcium current traces from three cells illustrating inhibition induced by (*b*) 10 nM, (*c*) 0.3 μM, or (*d*) 3 μM mapacalcine. *a*, Control calcium current before toxin application.

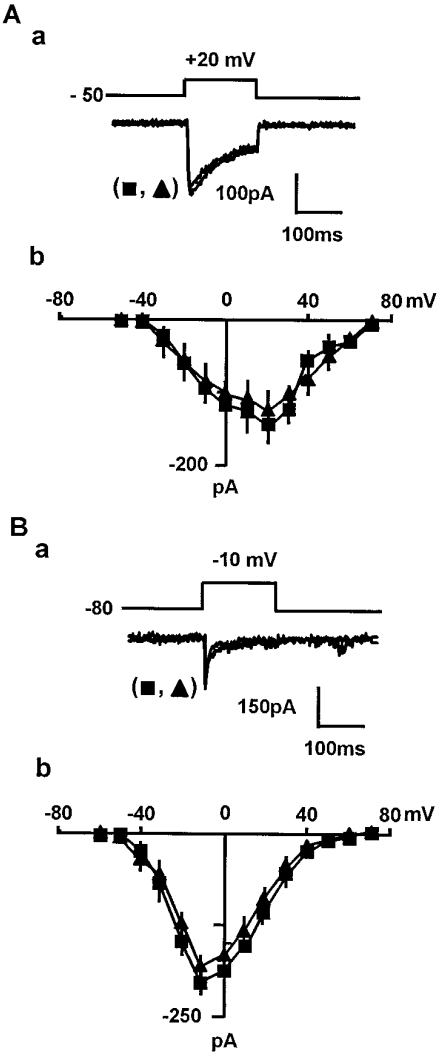

Fig. 7. Effects of mapacalcine on the L-type and T-type calcium currents in portal vein myocytes. A, L-type calcium currents elicited from a holding potential of −50 mV at a stimulation frequency of 0.05 Hz. *a*, Maximal calcium current in the (■) absence or (▲) presence of 3 μM mapacalcine. *b*, Current-voltage relationships obtained in the (■) absence or (▲) presence of 3 μM mapacalcine for 5 min. B, T-type calcium currents elicited from a holding potential of −80 mV at a stimulation frequency of 0.1 Hz for 10 min. *a*, Maximal calcium current in the (■) absence or (▲) presence of 3 μM mapacalcine. *b*, Current-voltage relationships obtained in the (■) absence or (▲) presence of 3 μM mapacalcine for 5 min.

In portal vein myocytes, L- and T-type calcium channels have been identified by using both electrophysiological and pharmacological experiments (7). Mapacalcine had no effect on both L-type calcium current (elicited from −50 mV at a stimulation frequency of 0.05 Hz) and T-type calcium current (elicited from −70 mV at a stimulation frequency of 0.1 Hz for 10 min), as shown in Fig. 7. These results indicate that mapacalcine selectively inhibits the non-L-type calcium current of duodenal myocytes.

Mechanisms of mapacalcine inhibition. A standardized protocol was used to assess the relative contribution of initial, conditioned, and tonic blockade of non-L-type calcium current by mapacalcine. As shown in Fig. 8A, the steady state inhibitory effect of 0.3 μM mapacalcine on the calcium current elicited by depolarizations from −80 mV to 0 mV, at a stimulation frequency of 0.1 Hz and in the presence of 10 μM oxodipine, was obtained within 4–6 min. The effects of mapacalcine was partially reversed after a 8–10-min return to reference solution. In Fig. 8B, a train of depolarizing pulses at 0.1 Hz was applied for 10 min, followed by a rest period of 4 min during which mapacalcine (0.5 μM) was perfused. A second identical voltage-clamp depolarization train was then applied. Blockade was estimated by measuring the difference in peak calcium current between control and test drug conditions when steady state blockade was obtained. The initial blockade, assessed as the difference in peak calcium current between the control and the first pulse after drug exposure, was 62 ± 5% (five experiments). Conditioned blockade was the difference between the peak calcium current for the first and the last pulses after drug exposure without rest period (Fig. 8C). The calcium current inhibition was 65 ± 8% (five experiments) and not different from that observed after a 4-min rest period ($p > 0.05$). Increasing the stimulation frequency from 0.1 to 0.2 Hz had no significant effect on the time course and steady state inhibition of calcium current in the presence of mapacalcine (67 ± 12%, six experiments; Fig. 8C). Tonic blockade was defined as the blockade of calcium current that could not be removed during a 2-min hyperpolarization at −100 mV. Because hyperpolarization of the membrane did not restore the calcium current (six experiments), we can postulate that the mapacalcine-induced blockade was largely tonic.

The next possibility was that membrane depolarization could alter the effectiveness of calcium current blockade by mapacalcine. The influence of mapacalcine on the voltage-dependent inactivation of the non-L-type calcium current was examined with the two-pulse protocol. In the presence of 0.3 μM mapacalcine, the inactivation curve was not modified (Fig. 8D), indicating no detectable voltage-dependent blockade of mapacalcine on this calcium current.

Effects of mapacalcine on other ionic channels. Voltage-activated potassium currents of duodenal and portal vein myocytes were obtained during depolarizations elicited from a holding potential of −80 mV. The cells were incubated for 20 min in 5 mM $BaCl_2$, and the pipette solution contained 130 mM KCl. In the presence of 3 μM mapacalcine for 5 min, no significant effect was observed on the voltage-dependent potassium current at any potentials tested (Fig. 9).

Calcium-activated chloride current can be induced via calcium influx through voltage-dependent calcium channels or calcium release from intracellular stores in response to caffeine or norepinephrine applications, as previously shown in portal vein myocytes (24). At a holding potential of −50 mV, the normal response to external microejections of 10 mM caffeine, in both duodenal and portal vein myocytes, was a transient chloride current depending on a transient increase in cytoplasmic calcium concentration. Because several caffeine-induced currents and calcium responses that are similar in amplitude and duration can be obtained with a time interval between successive caffeine applications of 3 min (24), it is possible to study the effects of mapacalcine on chloride current and caffeine-induced calcium response. The caffeine-evoked chloride currents in portal vein myocytes were not significantly modified in the presence of 3 μM mapacalcine [−148 ± 21 pA (nine experiments) versus −132 ± 37 pA (nine experiments), $p > 0.05$] like the calcium responses [310 ± 76 nM (nine experiments) versus 276 ± 37 nM (nine experiments), $p > 0.05$; Fig. 10]. Similarly, caffeine-

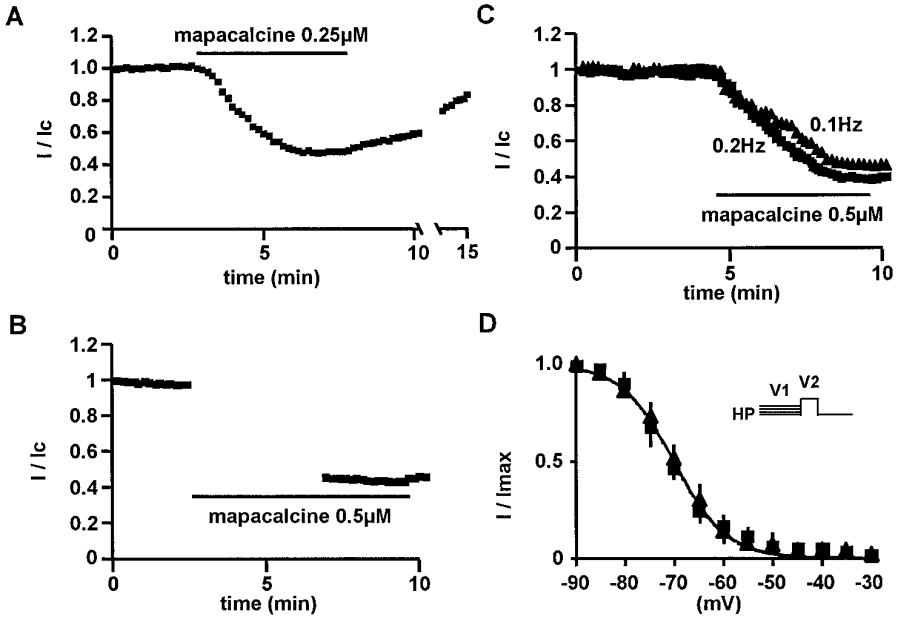

Fig. 8. Properties of mapacalcine inhibition. A, Time course of inhibition of the calcium current elicited from a holding potential of −80 to 0 mV at a stimulation frequency of 0.1 Hz for 10 min in the presence of 0.25 μM mapacalcine. B, Effect of frequency of command pulses on the calcium current before and after a rest period of 4 min in the presence of 0.5 μM mapacalcine. C, Command pulses applied at (▲) 0.1 Hz and (■) 0.2 Hz before and during application of 0.5 μM mapacalcine. D, Inactivation curve of the calcium current in the (■) absence or (▲) presence of 3 μM mapacalcine The test potential (V_2) is 0 mV, and the duration of the conditioning pulse (V_1) is 20 sec (*inset*). *Points,* mean response of 6−12 cells with the standard error shown (*vertical lines*). Calcium current was expressed as a fraction of control current (I/I_c) or maximal current (I/I_{max}).

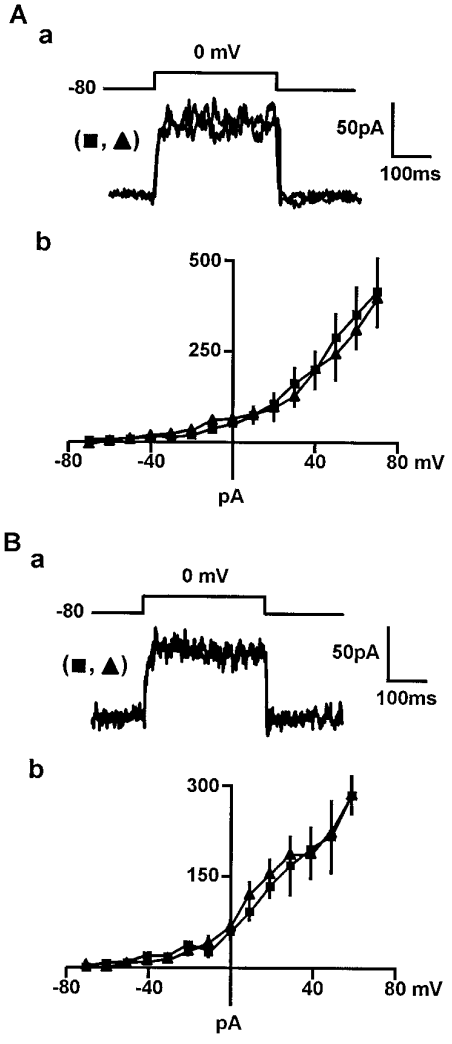

Fig. 9. Effects of mapacalcine on the voltage-dependent potassium currents in duodenal and portal vein myocytes. A, In duodenal cells, potassium currents evoked by a depolarization step to (*a*) 0 mV and (*b*) current-voltage relationships in the (■) absence or (▲) presence of 3 μM mapacalcine for 5 min, B, In portal vein cells, potassium currents evoked by a depolarization step to (*a*) 0 mV and (*b*) current-voltage relationships in the (■) absence or (▲) presence of 3 μM mapacalcine for 5 min.

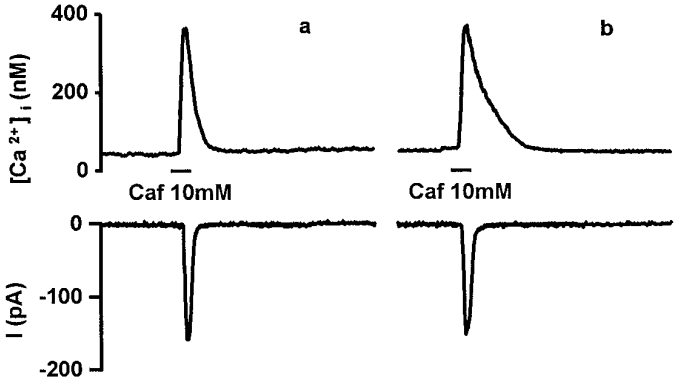

Fig. 10. Effects of mapacalcine on both calcium release and chloride current evoked by 10 mM caffeine in portal vein myocytes. *a*, Control conditions. *b*, In the presence of 3 μM mapacalcine for 5 min. The cells were voltage-clamped at a holding potential of −50 mV. The pipette solution contained 50 μM Indo-1.

evoked inward currents in mouse duodenal myocytes were not significantly modified in the presence of 3 μM mapacalcine [−108 ± 23 pA (10 experiments) versus −119 ± 25 pA (10 experiments), $p > 0.05$], like the calcium responses [295 ± 57 nM (12 experiments) versus 272 ± 61 nM (14 experiments), $p > 0.05$]. These results show that mapacalcine has no inhibitory effects on potassium or chloride currents and does not interact with the intracellular calcium stores.

Discussion

We demonstrate the existence of a new type of calcium channel coexisting along the typical L-type calcium channel in mouse duodenal smooth muscle cells. We also report the purification and characterization of a small protein from *C. vastifica* sponge that specifically blocks this calcium conductance.

The presence of several types of calcium channels in a same cellular type is a well-known situation (6–8). Even in visceral smooth muscle, the presence of both L-type and non-T/non-L-type calcium current has been suggested (9). Evidence supports that in mouse duodenal myocytes, the calcium current elicited by a depolarization from −80 mV (after complete blockade of L-type calcium channels) is a new type of calcium current, as follows. (a) This current is resistant to high stimulation frequency and to a variety of drugs, such as dihydropyridines, ω-conotoxin GVIA, ω-conotoxin MVIIC, and ω-agatoxin IVA, at the high concentrations used, indicating that it cannot be an L-, an N-, a P- or a Q-type calcium current. (b) The steady state inactivation curve is sigmoidal and voltage dependent. Half-maximal and complete inactivations are obtained at more negative potentials (−70 and −45 mV, respectively) than those of the L-type calcium current (−40 and −10 mV, respectively). (c) T-type calcium channels have been previously described in cardiac cells (25) and smooth muscle cells (7, 26). These channels are also activated when cells are maintained at a low holding potential, ~−70 mV, and are resistant to high stimulation frequencies. Although T-type calcium channels were first described as dihydropyridine-resistant channels (27), recent studies report a certain sensitivity to dihydropyridines like isradipine (7, 28) and antispasmodic drugs like fenoverine (29). The non-L-type calcium current of duodenal myocytes seems completely insensitive to high concentrations of fenoverine and isradipine. (d) The new toxin, mapacalcine, selectively inhibits the non-L-type calcium current of duodenal myocytes. Mapacalcine has no effect on L-type calcium channels, potassium, or chloride channels in duodenal and portal vein myocytes. (e) Mapacalcine does not affect the calcium responses induced by caffeine, suggesting that it does not interact with the intracellular calcium stores. (f) The time constants of inactivation for the non-L-type calcium current in duodenal myocytes are slow compared with the fast inactivation decay of the T-type calcium current in other cell types (27). This may be due to the fact that the slow time constants of inactivation are very insensitive to changes in membrane potential and that only the fast time constants follow a bell-shaped curve against voltage. Another type of calcium channels, the R-type channel, has been recently described in neuronal tissues as a high voltage-activated calcium channel that is insensitive to the pharmacological drugs

used in this study (15). However, this calcium current inactivates faster than the non-L-type calcium current of duodenal myocytes (30). Until now, R-type calcium channels have not been found in peripheral excitable tissues, and it is unlikely that the calcium conductance described in this work could correspond to a peripheral form of the R-type calcium channel. According to our data, mapacalcine seems to be very specific for a new type of calcium current, identified in duodenal myocytes. This current is activated at membrane potentials near −60 mV, has a slow inactivation decay, and is resistant to rundown by a high stimulation frequency and a variety of calcium channel blockers.

Our structural data show that mapacalcine is a dimeric protein composed of two identical chains of 9541 Da (corresponding to its reduced monomer with amidated carboxyl terminus). The amino acid sequence of a mapacalcine monomer does not show significant homologies with protein sequences in data banks. The polymeric structure of certain toxins seems to be associated with membrane insertion and channel-forming properties. For example, the mechanisms of action of aerolysin, a peptide secreted by *Aeromonas hydrophyla*, have been described. Aerolysin is secreted as a dimeric prototoxin able to cross the bacterial membranes; after proteolytic processing, it forms an heptamer that is able to insert into the cellular membrane and form a voltage-gated anion-selective channel (31, 32). The ant toxin, ectatomin, a 7928-Da peptide, is formed by two highly homologous polypeptide chains linked by a disulfide bond. It forms a bundle of four amphipatic α helices in aqueous solution (33). In its dimeric state and at concentrations of 10–50 μM, this toxin is able to form a potential-dependent nonselective cation channel in cell membranes (33). Although pore-forming peptides have been isolated from marine sponges (34), the mechanisms of action of mapacalcine cannot be attributed to a channel-forming activity, which could be expected with respect to its dimeric structure comparable to that of ectatomin. Our data clearly show that no leak current appears in the presence of mapacalcine. On the contrary, we observed a specific calcium current blockade. Mapacalcine seems, by the way, to be the first toxin sharing some structural properties of the family of channel-forming toxins but does not obviously act like them. It acts probably like classic channel-blocking toxins through direct interaction with the ionic channel or related proteins. Our experimental results are consistent with the binding of mapacalcine to resting calcium channels. Increasing the rate at which calcium channels are activated ($\leq$0.2 Hz) as well as the number of inactivated calcium channels at depolarized holding potentials does not affect the inhibitory action of mapacalcine (absence of use and potential dependence). Further experiments using a labeled derivative of mapacalcine will be performed to investigate the interactions between the toxin and its receptors. Subunitary composition of the protein associated to the calcium channel described here will have to be elucidated, allowing comparison with subunitary composition of already described calcium channels. Improvement in the knowledge of the mapacalcine-sensitive calcium channel should provide informations regarding its contribution in the treatment of intestinal diseases associated to perturbations of cellular calcium homeostasis.

References

1. Herken, H., and F. Hucho. *Handbook of Experimental Pharmacology: Selective Neurotoxicity.* Springer-Verlag, Berlin (1992).
2. Tsien, R. W., P. T. Ellinor, and W. A. Horne. Molecular diversity of voltage-dependent Ca^{2+} channels. *Trends Pharmacol. Sci.* **12:**349–354 (1991).
3. Bezprozvanny, I., and R. W. Tsien. Voltage-dependent blockade of diverse types of voltage-gated Ca^{2+} channels expressed in *Xenopus* oocytes by the Ca^{2+} channel antagonist mibefradil (Ro 40–5967). *Mol. Pharmacol.* **48:** 540–549 (1995).
4. Fleckenstein, A. *Calcium Antagonism in Heart and Smooth Muscle: Experimental Facts and Therapeutic Prospects.* John Wiley & Sons, New York (1983).
5. Hosey, M., and M. Lazdunski. Calcium channels: molecular pharmacology, structure and regulation. *J. Membr. Biol.* **104:**81–105 (1988).
6. Benham, C. D., P. Hess, and R. W. Tsien. Two types of calcium channels in single smooth muscle cells from rabbit ear artery studied with whole-cell and single-channel recordings. *Circ. Res.* **61:**I10–I16 (1987).
7. Loirand, G., C. Mironneau, J. Mironneau, and P. Pacaud. Two types of calcium currents in single smooth muscle cells from rat portal vein. *J. Physiol. (Lond.).* **412:**333–349 (1989).
8. Neveu, D., J. Nargeot, and S. Richard. Two high voltage-activated dihydropyridine-sensitive Ca^{2+} channel currents with distinct electrophysiological and pharmacological properties in cultured aortic myocytes. *Pflueg. Arch. Eur. J. Physiol.* **424:**45–53 (1993).
9. Vivaudou, M. B., J. Singer, and J. V. Walsh, Jr. Multiple types of Ca^{2+} channels in visceral smooth muscle cells. *Pflueg. Arch. Eur. J. Physiol.* **418:**144–152 (1991).
10. Smirnov, S. V., A. V. Zholos, and M. F. Shuba. Potential-dependent inward currents in single isolated smooth muscle cells of the rat ileum. *J. Physiol. (Lond.)* **454:**549–571 (1992).
11. Mintz, I. M., M. E. Adams, and B. P. Bean. P-type calcium channels in rat central and peripheral neurons. *Neuron* **9:**85–95 (1992).
12. Turner, J. T., M. E. Adams, and K. Dunlap. Calcium channels coupled to glutamate release identified by *omega*-Aga-IVA. *Science (Washington D. C.)* **258:**310–313 (1992).
13. Cruz, L. J., D. S. Johnson, and B. M. Olivera. Characterization of the *omega*-conotoxin target: evidence for tissue-specific heterogeneity in calcium channel types. *Biochemistry* **26:**820–824 (1987).
14. Takahashi, T., and A. Momiyama. Different types of calcium channels mediate central synaptic transmission. *Nature (Lond.).* **366:**156–158 (1993).
15. Wheeler, D. B., A. Randall, and R. W. Tsien. Roles of N-type and Q-type Ca^{2+} channels in supporting hippocampal synaptic transmission. *Science (Washington D. C.)* **264:**107–111 (1994).
16. Snutch, T. P., and P. B. Reiner. Ca^{2+} channels: diversity of form and function. *Curr. Opin. Neurobiol.* **2:**247–253 (1992).
17. Coue, M., S. L. Brenner, I. Spector, and E. D. Korn. Inhibition of actin polymerization by latrunculin A. *FEBS Lett.* **213:**316–318 (1987).
18. Gunasekera, S. P., S. A. Pomponi, and P. J. McCarthy. Discobahamins A, B: new peptides from the Bahamian deep water marine sponge *Discodermia* sponge. *J. Nat. Prod.* **57:**79–83 (1994).
19. Li, H., S. Matsunaga, and N. Fusetani. Halicylindramides D and E, antifungal peptides from the marine sponge *Halichondria cylindrata.* *J. Nat. Prod.* **59:**163–166 (1996).
20. Maryanoff, B. E., X. Qiu, K. P. Padmanabhan, A. Tulinsky, H. R. Almond, P. Andrade-Gordon, M. N. Greco, J. A. Kauffman, K. C. Nicolaou, A. Liu, P. H. Brungo, and N. Fusetani. Molecular basis for the inhibition of human *alpha*-thrombin by the macrocyclic peptide cyclotheonamide A. *Proc. Natl. Acad. Sci. USA.* **90:**8048–8052 (1993).
21. Busseau, L. J., A. A. Beveridge, R. Nadeson, and A. P. Anderson. The marine natural product 3,5-dibromo-2-(2,4-dibromo-phenoxy) phenol inhibits contractile activity in the guinea-pig ileum. *Clin. Exp. Pharmacol. Physiol.* **20:**697–704 (1993).
22. Morel, J. L., N. Macrez-Leprêtre, and J. Mironneau. Angiotensin II-activated Ca^{2+} entry-induced release of Ca^{2+} from intracellular stores in rat portal vein myocytes. *Br. J. Pharmacol.* **118:**73–78 (1996).
23. Weiland, G. A., and P. B. Molinoff. Quantitative analysis of drug-receptor interactions: determination of kinetic and equilibrium properties. *Life Sci.* **29:**313–330 (1981).
24. Baron, A., P. Pacaud, G. Loirand, C. Mironneau, and J. Mironneau. Pharmacological block of Ca^{2+}-activated Cl^- current in rat vascular smooth muscle cells in short-term primary culture. *Pflueg. Arch. Eur. J. Physiol.* **419:**553–558 (1991).
25. Brown, A. M., D. L. Kunze, and A. Yatani. The agonist effect of dihydropyridines on Ca^{2+} channels. *Nature (Lond.).* **311:**570–572 (1984).
26. Yoshino, M., T. Someya, A. Nishio, K. Yazawa, T. Usuki, and H. Yabu. Multiple types of voltage-dependent Ca^{2+} channels in mammalian intestinal smooth muscle cells. *Pflueg. Arch. Eur. J. Physiol.* **414:**401–409 (1989).
27. Nilius, B., P. Hess, J. B. Lansman, and R. W. Tsien. A novel type of cardiac calcium channel in ventricular cells. *Nature (Lond.)* **316:**443–446 (1985).
28. Dacquet, C., P. Pacaud, G. Loirand, C. Mironneau, and J. Mironneau. Comparison of binding affinities and calcium current inhibitory effects of

a 1,4-dihydropyridine derivative (PN 200–110) in vascular smooth muscle. *Biochem. Biophys. Res. Commun.* **152:**1165–1172 (1988).
29. Mironneau, J., S. Arnaudeau, and C. Mironneau. Fenoverine inhibition of calcium channel currents in single smooth muscle cells from rat portal vein and myometrium. *Br. J. Pharmacol.* **104:**65–70 (1991).
30. Ellinor, P. T., J. F. Zhang, A. D. Randall, M. Zhou, T. L. Schwarz, R. W. Tsien, and W. A. Horne. Functional expression of a rapidly inactivating neuronal calcium channel. *Nature (Lond.).* **363:**455–458 (1993).
31. Buckley, J. T. Crossing three membranes: channel formation by aerolysin. *FEBS Lett.* **307:**30–33 (1992).
32. Van Der Goot, F. G., J. Ausio, K. R. Wong, F. Pattus, and J. T. Buckley. Dimerization stabilizes the pore forming toxin aerolysin in solution. *J. Biol. Chem.* **268:**18272–18279 (1993).
33. Pluzhinikov, K. A., D. E. Nolde, S. M. Tertyshnikova, S. V. Sukhanov, A. G. Sobol, A. K. Torgov, A. Filippov, S. Arsenev, and E. V. Grishin. Structure activity study of the basic toxic component of venom from the ant *Ectatoma tuberulatum. Bioorg. Khim.* **20:**857–871 (1994).
34. Mangel, A., J. M. Leitao, R. Batel, H. Zimmerman, W. E. Muller, and H. C. Schroder. Purification and characterization of a pore forming protein from the marine sponge *Tethya lyncurium. Eur. J. Biochem.* **210:**499–507 (1992).

Send reprint requests to: Dr. Michel Hugues, CNRS ESA 5017, Physiopathologie et Pharmacologie Vasculaire, Université de Bordeaux II, 146 rue Léo Saignat, 33076 Bordeaux Cedex, France. E-mail: michel.hugues@hippocrate.u-bordeaux2.fr